OPTICAL WAVEGUIDE COMPONENTS

An optical waveguide is a conduit that guides the propagation of a light beam so that the power of the beam is confined in a controlled transverse direction. Optical waveguides are usually constructed by sandwiching a higher refractive index medium (referred to as a *core*) between lower refractive media (referred to as *cladding*). The optical properties of the waveguide can be altered either by applying an external perturbation such as an electrical bias or by tailoring the waveguide material or structure. Therefore, many different types of optical waveguide components can be designed, each performing one or several functions, such as emission (i.e., laser), modulation, transmission, distribution, and detection of a light signal. These various waveguide components can be combined to make integrated opto-electronic circuits or systems that use light (*photons*) as a carrier for the transmission and processing of signals. The realization of these systems revolutionized telecommunications and the microwave engineering field. This integrated optical system/network offers the advantage of much larger bandwidth or information-carrying capacity, miniature size, low power consumption, and negligible sensitivity to interference by natural or man-made electromagnetic field noise compared with older electrical systems. Integrated optical waveguide circuits not only have the potential to replace many electronic circuits and large conventional optical apparatus, but they also have applications that cannot be emulated by electronic counterparts.

Historical Perspectives

The earliest optical waveguide can be traced back to 1870, when John Tyndall demonstrated the guidance of an optical beam in a transparent cylindrical rod by multiple total internal reflection from the surface of the cylinder. However, a surge of interest in optical waveguides was stimulated by the technological advances of fiber optics, lasers, and semiconductor materials in the late 1950s and early 1960s, when the possibilities and advantages of fiber-optic communication were recognized. Kao et al. (1) performed early experiments to demonstrate the concept of fiber-optic communications, but the power loss of their optical fiber was approximately 3,000 dB/km. Kapany (2) documented and reviewed the early work and the basic principle of optical fibers. Planar or slab dielectric waveguides were first studied and used in the microwave regime. In 1965, Anderson et al. (3) used these concepts, combined with thin-film deposition and photolithographical techniques to create thin-film optical waveguides. The theoretical formalism for electromagnetic wave propagation in circular and planar optical waveguides was presented by Kapany and Burke (4), and Marcuse (5) in 1972.

In 1962 and 1963, several groups (6,7) observed lasing action in semiconductors at the same time as Yariv and Leite (8) reported guiding within planar layers of a p–n junction. Subsequently, these results led to the development of optical waveguide modulators and semiconductor heterostructure waveguide lasers (7), which combined a p–n junction with a cladding/core/cladding waveguide structure. Based on this and other earlier optical waveguiding research, S. E. Miller (9) of Bell Laboratories proposed the concept of *integrated optics* in 1969. This concept launched a massive theoretical and experimental research effort in the field of optical integrated circuits (10,11). These studies started with hybrid integration of active waveguide components such as lasers, amplifiers, or detectors with passive dielectric optical waveguides. A large number of optical waveguide materials such as glass, $LiNbO_3$, semiconductors, and polymers were evaluated at that time.

In the late 1970s, optical-fiber transmission loss was reduced to 0.2 dB/km (1) and GaAs-based semiconductor laser-diode performance was significantly improved, accelerating the development of optical fiber communication systems. However, the low dispersion and low-loss wavelength regions are at 1.3 μm and 1.55 μm, respectively, therefore in the early 1980s most laser diode research was refocused on InGaAsP-InP 1.3 μm and 1.55 μm lasers. In the 1980s, optical fiber communication systems started to be commercialized, and digital fiber-optic links for telephone communications were realized in many countries.

In order to increase information transmission capacity, increasing the modulation frequency became an important issue. There are two approaches, direct laser modulation and high-speed waveguide modulation. The maximum modulation frequency has been continuously increased from a few gigahertz (GHz) in the mid-1980s to around 50 GHz in the early 1990s (12,13). Since direct laser modulation has a fundamental limit around 30 GHz and additional wavelength chirping (which is a wavelength drift caused by the laser cavity's condition change during direct modulation), subsequent work focused on semiconductor quantum well waveguide modulators integrated with high quality lasers, such as distributed feedback (DFB) lasers and distributed Bragg reflector (DBR) lasers (13). Meanwhile, other related waveguide devices, such as optical switches, splitters, and couplers, were developed for the communication networks. To further increase the information transport capacity, two new approaches were developed since 1990. The first approach is to increase the rate of data transmission on the network through time division multiplexing (TDM) of signals from multiple sources. This method requires the use of laser pulses with very short duration, on the order of picoseconds, and high-speed switching components for multiplexing and demultiplexing. A major setback in this approach is that the short optical pulses tend to broaden as they propagate through the optical fiber or other optical waveguides. This broadening is a result of the dispersion of the waveguide material and causes the different section of an optical pulse to travel with a slightly different velocity. Researchers are also working on a variant of TDM by employing very short laser pulses to produce solitons in optical fibers. Solitons are optical pulses that are temporally shaped in such a manner that they propagate through an optical fiber without changing in amplitude or shape. This phenomenon occurs because glass, like most other waveguide material, is nonlinear, i.e., its refractive index changes in response to varying optical intensity. With use of this technique, optical pulses can be transmitted over hundreds of kilometers without re-amplification. A second, more popular approach was to develop a wavelength division multiplexing (WDM) network that used multiple lasers with different wavelengths to transmit multiple signals through an optical

fiber, thereby increasing the number of carriers available for signal transport (14). Extensive research on WDM has continued with the successful development of a new type of waveguide component that can combine, divide, switch, and redistribute laser beams according to wavelength.

Like the modern silicon-semiconductor industry, the success of the waveguide photonic system relies on monolithic integration. Integrated optical waveguide circuits have been under intense study for telecommunication networks, computer network links, optical computing, RF (radio frequency) spectrum analyzers, laser radar, optical gyroscopes, optically controlled microwave, and so on.

Overview of Optical Waveguide Components

A simple method of categorizing optical waveguide components is by active or passive function. Active devices perform dynamic optical-wave control. Passive devices only exhibit static characteristics for optical waves. One can also classify optical waveguides into categories by their geometry (i.e., slab, cylindrical rod, fiber optic, ridge waveguide), by material composition, or by any other waveguide physical parameter. However, since the optical fiber represents a large topic, it is common practice to consider optical fibers separately from optical waveguide components, and therefore a detailed discussion of optical fibers will not be included in this article.

Active optical waveguide components, also referred to as functional waveguide devices, require an external field such as an electrical bias or a second light beam to dynamically perturb the light propagation or convert energy in the waveguide. The active waveguides can be further subdivided into two groups. The first group includes waveguide lasers, amplifiers, waveguide light-emitting diodes (LED), super luminescent diodes, and wavelength converters. These devices generate light in the waveguide by spontaneous or stimulated emission exhibiting optical gain and will be discussed later in this article. The second group includes waveguide modulators (for amplitude, phase or polarization modulation), phase shifters, switches, polarization controllers, and detectors. These devices do not exhibit optical gain; however, the light is perturbed by using some physical effects, such as the electro-optic, electro-refractive, quantum Stark, electro-absorption, plasma, nonlinear-optic, magneto-optic, acousto-optic, or thermo-optic.

Passive optical waveguide components direct or distribute lightwaves by guiding, reflecting, or diffracting them in a controlled manner. Therefore, passive devices exhibit static characteristics for the electromagnetic wave, and do not require any external field to operate the device. These components include optical path-bends, optical beam splitters/dividers, combiners/multiplexers, couplers, polarizers, mode splitters, waveguide lenses, wavelength demultiplexers, or simple transparent waveguides. The characteristics of these devices will be discussed in the waveguide theory section.

Overview of Optical Waveguide Materials and Fabrication Techniques

Many materials have been evaluated and used for optical waveguides. Most can be classified into three basic material groups: dielectrics, semiconductors, and polymers. Optical waveguides are fabricated on a host substrate that belongs either to the same or a different material group. The most commonly used waveguide and substrate materials are given in Table 1.

Dielectric waveguides, such as $LiNbO_3$ and glass waveguides, have the advantage of index matching with the optical fiber and very low absorption and insertion loss. However these materials have a large energy band gap compared with the operating light energy, making them untenable for active devices with optical gain or absorption. Semiconductor waveguides, however, can be designed for all types of active optical components, for passive optical components, and for electronic devices, so they are ideally suited for fully monolithic integrated optical waveguide circuits/systems. In addition, semiconductor material systems have the advantage of larger flexibility and control in terms of material compositions, bandgap engineering, and so on. However, the absorption and insertion losses are larger than in the dielectric waveguide. Polymer waveguides are relatively inexpensive to fabricate and are commonly used for making interconnections between two types of waveguide components. Additionally, active waveguide devices have been made with polymer material in many laboratories.

A large variety of methods exist for the fabrication of optical waveguides. These processing techniques vary from thick film to thin-film processing. Figure 1 shows some simple representations of typical waveguides. Figure 2 shows a sequential diagram of processing techniques used to achieve the structures shown in Fig. 1 for different materials. In general, the first fabrication step is to form the thin-film layers that define the cladding/core/cladding waveguide in a vertical direction. For dielectric waveguides, several deposition methods exist for forming the thin-film layers including sputtering, vacuum-vapor deposition, chemical vapor deposition (CVD), and plasma deposition. The layered semiconductor materials are grown by molecular beam epitaxy (MBE) or metal-organic chemical vapor deposition (MOCVD). The polymer films are

Table 1. Commonly Used Optical Waveguide Materials

Top Cladding	GaAlAs	InP	InAlAs	Air	SiO_2 Glass	Air	Polymer
Core	(In)GaAs/ GaAlAs	InGaAs/ InGaAsP	InGaAs/ InGaAlAs	$LiNbO_3$ (Ti or LiO_2 diffusion)	SiO_2 Glass	$LiTaO_3$ (Cu, Ti, Nb)	Polymer
Bottom Cladding	GaAlAs	InP	InAlAs	$LiNbO_3$	SiO_2 Glass	$LiTaO_3$	Polymer
Substrate	GaAs	InP	InP	Glass, SiO_2/Si $LiTaO_3$	SiO_2/Si, GaAs, InP	$LiTaO_3$	Glass, Si, GaAs, InP

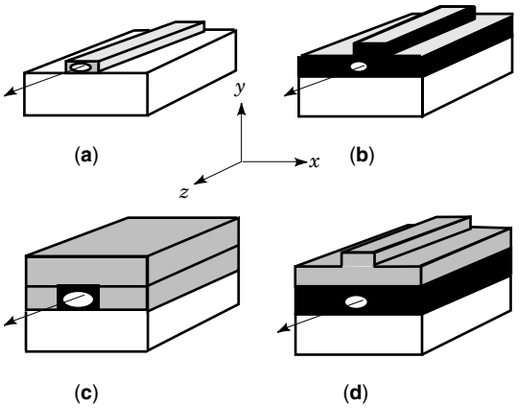

Figure 1. Schematic representation of four typical simple waveguide geometries. (a) Strip. (b) Ridge. (c) Buried ridge. (d) Strip loaded.

created by liquid-source deposition such as spin coating followed by bake/cure cycles. The second step of processing is to laterally define the channeled waveguide. To form ridge waveguides, the conventional method is photolithography (masking) and etching, as shown in Fig. 2. For embedded strip waveguides, the fabrication techniques are diffusion, ion-implantation, or ion-exchange, with masking by photolithography. Step three is to make electrical contacts for active devices. This involves the deposition of dielectric isolation layer (for vertical direction electric isolation), ion-implantation for lateral electric isolation, and metal contact deposition/annealing. More details of these waveguide growth and fabrication techniques can be found in textbooks by Nishihara et al. (10), by Hunsperger (11), and in a book edited by Sze (15).

WAVEGUIDE THEORY

Optical Confinement and Waveguide Modes

Waveguide Modes. The basic concept of optical confinement is quite simple. A medium of higher refractive index is embedded in a medium of lower refractive index acting as a light

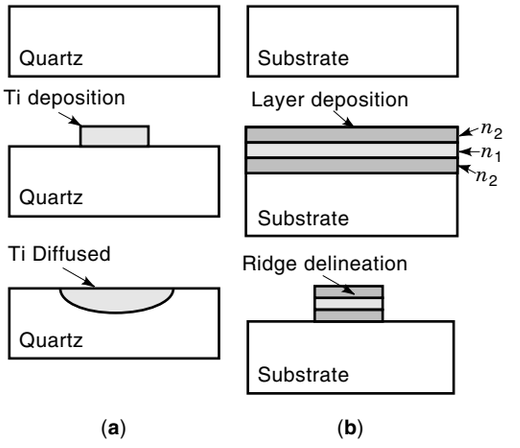

Figure 2. Typical optical waveguide fabrication sequence for (a) Quartz. (b) Semiconductor or glass substrates.

"trap" within which optical rays remain confined due to multiple total internal reflections at the boundaries, thus guiding the light from one location to another. Although one could analyze light-guiding phenomenon as a superposition of many plane waves propagating through the guide, such an analysis is tedious. For a better description, a set of elementary waves that propagate along a waveguide with a well-defined phase velocity, cross-sectional intensity distribution, and polarization are defined. These elementary waves are called the modes of the waveguide. The electric and magnetic fields of a mode are of the form $u(x, y)\, e^{-j\beta z}$, where the z is the propagation axis of the waveguide, $u(x, y)$ is the transverse field distribution, and β is the propagation constant. The electric and magnetic fields must satisfy Maxwell's equations in all media that comprise the waveguide as well as all the boundary conditions of the structure. Thus, each mode is an eigenstate of Maxwell's equations and all modes of a waveguide are orthogonal to each other. Since the mode is determined by the waveguide structure, it does not depend on the source of the excitation. However, it should not be interpreted that guided light in a waveguide must be one of the modes. In fact, a field satisfying Maxwell's equations and the boundary conditions of the waveguide, even though it is not in the form of $u(x, y)\, e^{-j\beta z}$, can be guided in the waveguide. In mathematical terms, it can be considered as a superposition of the modes in that waveguide.

Ray-Optics Approach. Ray-optics provides a simple picture with great intuitive appeal, although not as complete a description as that provided by electromagnetic theory. Ray-optics provides the basic concepts and terminology, especially for a planar waveguide.

In ray-optics, the physical picture of guided light propagation is that light rays, making angles ($\pm\theta$) with the y axis, undergo multiple total internal reflections and travel in zig-zag fashion through the higher index media (shown in Fig. 3). More precisely, it is a picture of two superimposed plane waves with each of their wavenormals along one of two directions in the zig-zag path. The sum of two such waves with equal amplitudes and proper phase shift forms an electromagnetic field of a form of $u(x, y)\, e^{-j\beta z}$. However, not all the θs correspond with a physical mode. First, rays making angle θ smaller than the critical angle ($\pm\theta_c$) refract, losing a portion of their power at each reflection, and eventually vanish. Second, in order to keep only two distinct plane waves in the waveguide through multiple reflections, we have to impose a

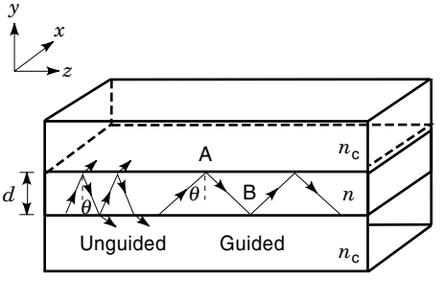

Figure 3. Zig-zag ray picture for modes in planar dielectric waveguide. Guided light propagation is that light rays, making angles ($\pm\theta$) with the y axis, undergo multiple total internal reflections and travel in zig-zag fashion through the higher index media.

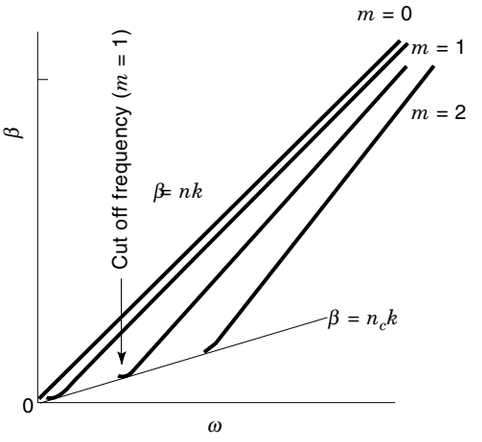

Figure 4. Typical dispersion relation (β-ω) for dielectric waveguides.

self-consistency condition, that is, requiring that as the zigzag wave reflects twice, it reproduces itself so that we have only two plane waves. This results in a self-consistency equation (16,17),

$$2nk\,d\cos\theta - 2\varphi = 2m\pi, \qquad m = 0, 1, 2, 3\ldots \tag{1}$$

Where $k = 2\pi/\lambda$ is the wavenumber of the plane waves, λ is the wavelength in vacuum, d is the thickness of the higher reflective index layer with a reflective index of n, and φ is the Goos-Hanchen phase shift that occurs on total internal reflection at the dielectric boundary.

Dispersion and Number of Modes. Equation (1) shows that for a given frequency and a given waveguide structure, only a discrete set of angles θ is allowed. Since $\beta = nk \sin\theta$, only a discrete set of β is allowed. Equation (1) is essentially a dispersion equation which yields the propagation constant β as a function of frequency ω. To satisfy Eq. (1), β is bounded by the plane wave propagation constants of the cladding and guiding layers: $n_c k < \beta < nk$, where n_c is the refractive index of the cladding layers. It is sometimes convenient to use an "effective guide index" defined as $N = \beta/k = n \sin\theta$ to describe the mode, which is bounded by $n_c < N < n$.

Figure 4 shows a typical dispersion relation between β and ω for a dielectric planar waveguide. The number of allowed modes is determined by the maximum allowed integer number of m which makes $n_c k < \beta < nk$. As shown in Fig. 4, the number of modes increases (decreases) with the increasing frequency (decreasing wavelength). The shortest frequency (longest wavelength) that can be guided by the structure is called the cutoff frequency (wavelength). Each mode has its own cutoff frequency (wavelength). If only one mode is allowed in the interested frequency range, the structure is said to be a single-mode waveguide. This occurs when the slab is sufficiently thin or the wavelength is sufficiently long. It can be proven that the number of modes is approximately proportional to the ratio of the thickness of the higher index layer to the wavelength, and to the numerical aperture (NA) of the waveguide, where $\mathrm{NA} = (n^2 - n_c^2)^{1/2}$ is the sine of the angle of acceptance of rays from air into the waveguide (17).

TE and TM Modes, Field Distribution. In a planar waveguide, the total internal reflection will not mix waves polarized either parallel or perpendicular to the plane of incidence. Therefore, transverse electric (TE) polarization and transverse magnetic (TM) polarization must satisfy the self-consistency condition independently. In the full electromagnetic theory, this means that TE and TM waves must each be capable of satisfying the boundary conditions. The modes with TE (TM) polarization are called TE (TM) modes. The nonvanishing field components for TE and TM modes in a planar waveguide are E_x, H_y, H_z and H_x, E_y, E_z, respectively (see Fig. 3).

The electromagnetic field of the TE mode inside the higher index layer of a symmetric planar waveguide is composed of the sum of the two plane waves with equal amplitudes and a phase shift $m\pi$ at the center of the slab. The complex amplitude of the nonvanishing electric field is $E_x = a_m u_m(y) \exp(-j\beta_m z)$ with (17)

$$u_m \propto \begin{Bmatrix} \cos\left(\dfrac{2\pi}{\lambda}\cos\theta_m y\right) & m = 0, 2, 4 \\ \sin\left(\dfrac{2\pi}{\lambda}\cos\theta_m y\right) & m = 1, 3, 5 \end{Bmatrix} -\frac{d}{2} < y < \frac{d}{2} \tag{2}$$

The component outside the higher index layer is an evanescent wave

$$u_m \propto \begin{Bmatrix} \exp(-\gamma_m y) & y > \dfrac{d}{2} \\ \exp(\gamma_m y) & y < -\dfrac{d}{2} \end{Bmatrix} \tag{3}$$

with $\gamma_m = n_c k(\sin^2\theta/\sin^2\theta_c - 1)^{1/2}$ the extinction coefficient. Similar results can be obtained for the TM mode by replacing E_y with H_y.

Group Velocity. The group velocity (v) for a pulse of light with an angular frequency centered at ω is given by $d\omega/d\beta$. In a planar waveguide, it is (17)

$$v = \frac{d\,\tan\theta + \Delta z}{d\,\sec\theta/c + \Delta\tau} \tag{4}$$

with c being the speed of light in the higher index media. In Eq. (4), $d \tan\theta$ is the distance the wave travels in the z direction as a ray travels from point A to point B, which takes a time $d \sec\theta/c$, and $\Delta z = \partial\varphi_r/\partial\beta$ is the additional distance due to Goos-Hanchen effect in the total internal reflection, which lasts a time of $\Delta\tau = (\partial\varphi_r/\partial\omega)$. The above relation shows that different modes have different group velocity.

Each mode travels with a fixed group velocity. Therefore, its transverse intensity distribution is invariant with propagation. An arbitrary field traveling in a waveguide is the sum of many different modes. Since different modes have different group velocities, the sum field changes its transverse intensity distribution though the waveguide. Figure 5 illustrates how the transverse intensity distribution of a single mode is invariant to propagation, whereas the multimode distribution varies with z.

Two-Dimensional Waveguide. In practice, most waveguides are two dimensional, that is, they confine light in the two transverse directions (x and y directions). Figure 1 shows some useful two-dimensional waveguide geometries. Although the principle of operation and the underlying modal

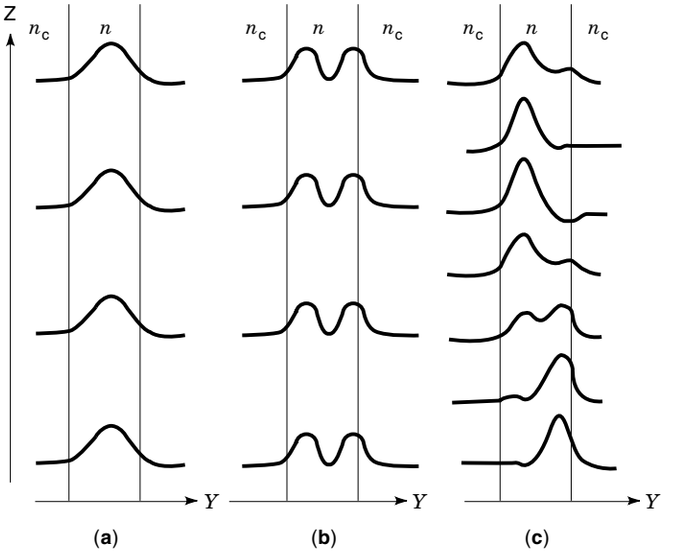

Figure 5. Transverse intensity distributions with respect to z in multimode waveguide. (a) Intensity distribution of $m = 1$ mode is invariant; (b) of $m = 2$ mode is also invariant; and (c) mixture of mode 1 and mode 2, intensity distribution changes with z.

structure of a two-dimensional waveguide is basically the same as a planar waveguide, the mathematical description for the two-dimensional structure is more complicated. It usually requires the solution of differential equations, that is, a reasonable amount of computer power. Therefore, considerable work has focused on approximations (18) such as the effective index method (EIM) and Marcatili's method. With increasing computing power, numerical solutions such as finite element (FE), finite difference (FD) and method of lines (MoL) algorithms has been used to analyze waveguide structure.

Marcatili's approach (18) is for a weakly guiding waveguide with a separable dielectric (or index) profile of $\epsilon = \epsilon_0 + \Delta\epsilon(x) + \Delta\epsilon(y)$. The two-dimensional waveguide is then considered as two planar waveguides in the x and y directions. The number of modes is equal to the product of the number of modes in the two planar waveguides and the field distribution associated with those modes is the product of the two corresponding field distributions.

In the effective index approximation (18), we project the refractive index $n(x, y)$ of a two-dimensional waveguide to the y axis. The projected refractive index at position $y = y_0$ is defined as the effective guide index $N(y_0)$ of a planar waveguide consisting of waveguide layers of $n(x, y_0)$ stacking along the x direction. After projection, we regard it as a slab waveguide stacking along the y direction with a refractive index profile of $N(y)$, and we finally solve the one dimensional problem. This approach is very efficient and has become one of the workhorses for design and modeling.

Optical Coupling and Beam Propagation in Waveguide

Mode Excitation. In the mode analysis, light propagating in a waveguide is in the form of many modes. The complex amplitude of optical field is a superposition of these modes (17):

$$E(x, y, z) = \sum_m a_m u_m(x, y) \exp(-j\beta_m z) \tag{5}$$

where a_m is the amplitude of mode m with a transverse distribution of $u_m(x, y)$ and a propagation constant of β_m. The amplitudes of the different modes depend on the nature of the light source used to excite the waveguide. If the source has a distribution that matches perfectly with that of a specific mode, only that mode is excited. A source of arbitrary distribution $s(x, y)$ excites different modes by different amounts. The fraction of the power transferred from the source to mode m depends on the degree of similarity between $s(x, y)$ and $u_m(x, y)$. The amplitude to the excited mode m is given by

$$a_m = \iint s(x, y) u_m(x, y) dx dy \tag{6}$$

Coupling Between Waveguides. If two waveguides are sufficiently close such that their fields overlap, light can couple from one into the other, an effect that can be used to make optical couplers and switches. Figure 6 shows the coupling between two parallel planar waveguides.

The formal approach (18) to study such a structure is to solve Maxwell's equations. However, finding a computer-generated solution for each particular geometry of interest is a tedious proposition which usually does not provide design guidance. For weak coupling a simplified approximation known as coupled mode theory is usually satisfactory.

The coupled mode theory (17) assumes that the modes of each of the waveguides remain approximately the same, say $u_1(x, y) \exp(-j\beta_1 z)$ and $u_2(x, y) \exp(-j\beta_2 z)$ for waveguide 1 and 2, respectively. The coupling modifies the amplitudes a_1 and a_2 of these modes of waveguide 1 and 2 such that they are functions of z. These two z-dependent amplitudes, $a_1(z)$ and $a_2(z)$, satisfy two differential equations:

$$\begin{aligned} \frac{da_1(z)}{dz} &= -jK_{21} \exp(j\Delta\beta z) a_2(z) \\ \frac{da_2(z)}{dz} &= -jK_{12} \exp(-j\Delta\beta z) a_1(z) \end{aligned} \tag{7}$$

where $\Delta\beta = \beta_1 - \beta_2$ and K_{21} and K_{12} are the coupling coefficients determined by the overlap of u_1 and u_2. Fig. 6(b) shows

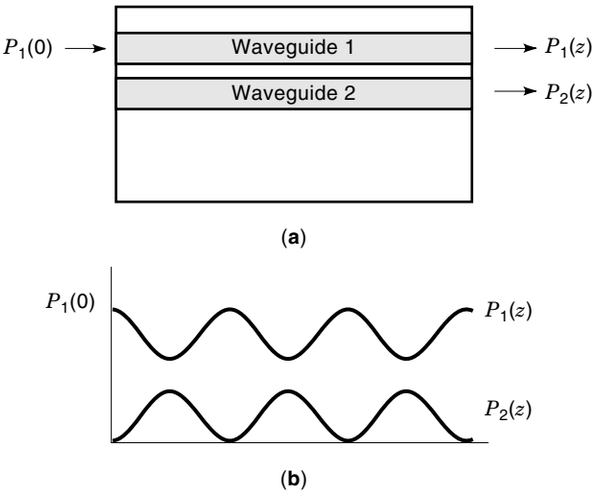

Figure 6. Exchange of power between two coupled waveguides. The coupling modifies the amplitudes of the modes in the two waveguides such that they are functions of z. The power is exchanged periodically between the two guides.

a typical solution, where the power is exchanged periodically between the two guides.

Local Modes, Adiabatic, and Abrupt Transitions. The concept of a mode is only valid for a structure whose cross section does not vary in the direction of optical propagation. In practice, waveguide structures vary in the direction of mode propagation. Figure 7 shows some useful waveguide configurations. Horns are used to change the dimensions of the channel waveguide; the Y-splitter plays the role of a beamsplitter or combiner; two Y-branches make a Mach–Zehnder interferometer, and directional couplers can be used to exchange optical power between waveguides.

Although we can not strictly speak of modes for the entire structure, we can speak of local modes at a particular position $z = z_0$. Local modes (19) are defined as the modes of a structure which take the waveguide parameter at $z = z_0$ as if it did not vary with z. It shall be noted that local mode is a function of z. The amplitudes of the local modes in a varying waveguide structure are not necessarily constant. Power transfer between the local modes depends on the rate of change of the geometry of the structure.

If the transition between two waveguide structures takes place gradually, the power transfer between the modes can be neglected. Although the local mode may change its shape in the process of modal evolution, coupling to the other local modes is assumed not to occur. This kind of transition is called an adiabatic transition (19). An example of this is the waveguide horn in which power coupled in the first-order local mode will end up in the first-order local mode [Fig. 8(a)].

The opposite extreme is an abrupt transition, in which a transition between two waveguide structures is made so abruptly that the maximum amount of power transfers between the local modes (19). The fraction of the power transferred from the local mode in the first structure to the local mode in the second depends on the degree of similarity between them. Figure 8 shows a directional coupler. At the starting point of the coupled waveguide section ($z = 0$), an abrupt transition occurs. The first-order local mode in one of the two branches excites two local modes in the coupled waveguide section. At the ending point ($z = L_c$), another abrupt transition occurs. The two local modes in the coupled waveguide section excite two local modes in the two exit branches. The amplitude of these two modes depends on the length (L) of the coupled section.

Beam Propagation Method. Beam propagation method (BPM) is a useful and powerful computer simulation method for waveguide modeling. Different from mode analysis, BPM is not a constructive method. BPM yields the response of a given device to an external optical signal.

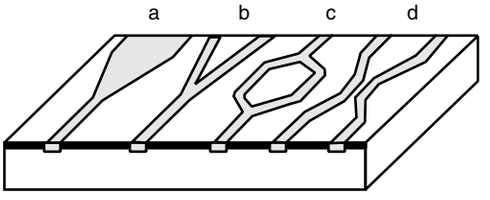

Figure 7. Some useful waveguide structures: (a) horn; (b) Y-splitter; (c) Mach–Zehnder; and (d) directional coupler.

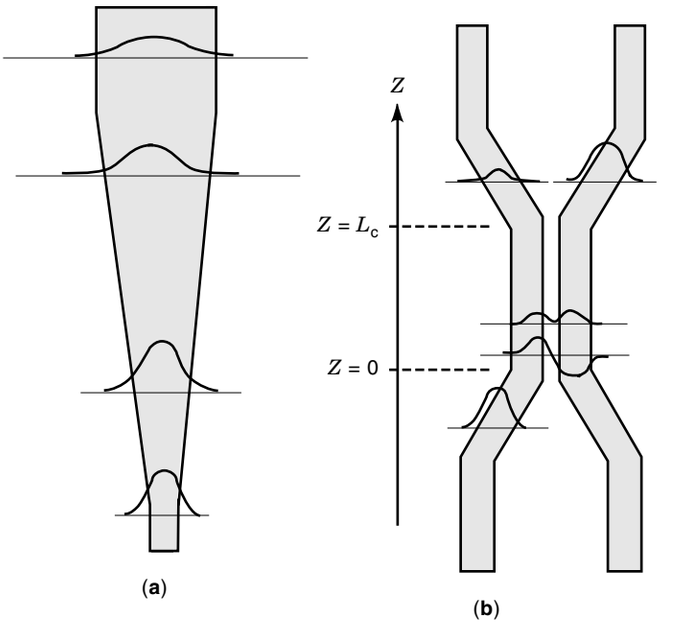

Figure 8. Local modes and mode transitions: (a) adiabatic transitions in horn; (b) abrupt transitions at start and end points of directional coupler.

In the classical BPM (17), the propagation of an optical beam in an inhomogeneous medium is replaced by a sequence of free-space propagation steps and phase corrections. In dramatic terms, the input beam knows nothing about the inhomogeneities located in the step until it finishes a half-step. Then the entire information about the inhomogeneities in the step is replaced by a single phase correction. Afterward, the beam finishes the other half-step without being influenced by any inhomogeneity. In some modern BPM algorithms, the local modes at the actual cross section of the waveguide are used to evaluate the particular BPM steps. Finite difference and finite element algorithms are also used in BPM. Readers are referred to Ref. 17.

WAVEGUIDE DEVICES FOR EMISSION, AMPLIFICATION, AND DETECTION

Waveguide devices can be categorized by their use as emitters, amplifiers, and detectors. While each of these categories encompasses more than waveguide devices, this section concentrates only on those devices that function primarily in the waveguide configuration or that have been adapted to the waveguide configuration. The first category introduced is emission which includes lasers and light emitting diodes (LED); the next category is semiconductor laser amplifiers, and finally, the last category is waveguide photodetectors.

Emission

A semiconductor laser and LED have a number of similarities and one glaring difference. The difference is that LED emission is dominated by spontaneous emission, while the laser is dominated by stimulated emission. Principal among the similarities is the use of a semiconductor p–n junction operated

Table 2. Recombination Rate Constant for Typical Semiconductors

Material	Direct/ Indirect Gap	Emission Wavelength (μm)	B (m^3s^{-1})
Si	Indirect	1.11	1.79×10^{-21}
Ge	Indirect	1.88	5.25×10^{-20}
GaAs	Direct	0.86	7.21×10^{-16}
GaP	Indirect	0.55	5.37×10^{-20}
InAs	Direct	3.54	8.50×10^{-17}
InP	Direct	0.92	1.26×10^{-15}

under forward bias. In this mode of operation, electrons and holes are injected into the p and n sides of the junction, respectively. The injected charge recombines in a process referred to as electroluminescence, results in the emission of a phonon with a wavelength that is inversely proportional to the band gap of the material. The rate of recombination is determined by the number of electrons and holes available and can be written as

$$r = Bnp \tag{8}$$

where n and p are the electron and hole concentrations, respectively, and B is a constant of proportionality. Table 2 lists this constant for some typical semiconductors. It is apparent from looking at Table 2 that direct band semiconductors have a much higher proportionality constant than do indirect semiconductors. Figure 9 shows a graph of wavelength as a function of different material systems. In some cases, it is possible to tailor the operating wavelength by choosing a ternary or quaternary combination of the constituent binaries shown in Fig. 9.

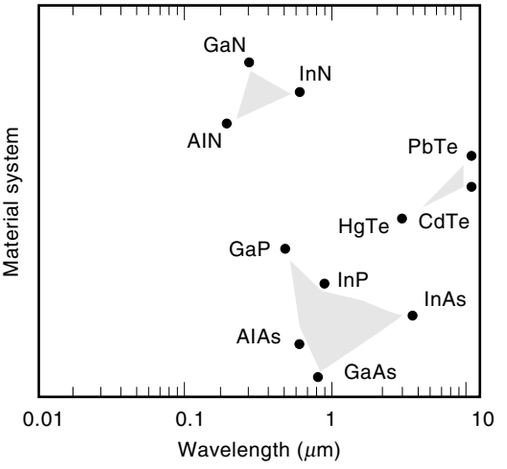

Figure 9. Emission wavelength ranges for some commonly used binaries. The shaded regions indicate wavelengths achieved by using a ternary or quaternary mix of the constituent binaries.

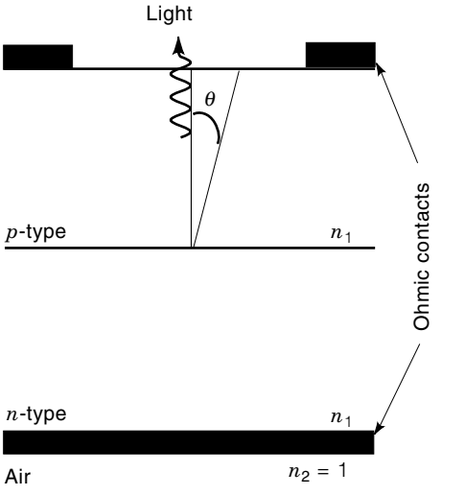

Figure 10. A simple, top illuminating light emitting diode (LED) structure.

Light Emitting Diodes. A simple LED structure is shown in Fig. 10. As it represents a simple p–n junction, the current-voltage characteristic is given by

$$I = qA\left[\frac{D_n n_i^2}{L_n N_A} + \frac{D_p n_i^2}{L_p N_D}\right][\exp(qV_a/k_B T) - 1] \tag{9}$$

where $D_{n,p}$ are defined by the Einstein relation,

$$\frac{D_{n,p}}{\mu_{n,p}} = \frac{k_B T}{q} \tag{10}$$

$L_{n,p}$ represents the extent of the injection into the p and n regions, respectively, and is equal to $\sqrt{D_{n,p}\tau_{n,p}}$, n_i^2 is the intrinsic carrier concentration, $N_{A,D}$ are the doping levels in the p and n regions, respectively, and V_A is the applied voltage. The internal quantum efficiency expressed as the fraction of electrons injected into the p side of the junction is given by

$$\eta = \left[1 + \frac{D_p L_n p_n}{D_n L_p n_p}\right] \tag{11}$$

In most cases, $\mu_n \gg \mu_p$, and assuming that $L_n \cong L_p$, the internal quantum efficiency tends toward unity; this does not mean that the efficiency of the LED is unity, in many cases, other recombination mechanisms arise that decrease the electrical to optical conversion efficiency.

If the emission from the LED junction is treated as a point source, then due to Snell's law, only the fraction of photons with an emission angle that is within the solid angle formed by θ will be able to escape the semiconductor surface. The efficiency due to this factor is given by the following equation:

$$\eta \approx \frac{1}{4}\left(\frac{n_2}{n_1}\right)^2\left[1 - \left(\frac{n_1 - n_2}{n_2 + n_1}\right)^2\right] \tag{12}$$

where n is the index of refraction as defined in Fig. 10. The problem with the LED in a standard configuration is that only a small portion of the light generated at the junction can es-

cape, which subsequently decreases the external quantum efficiency of the LED. One method of enhancing the LED is to sandwich the LED within a waveguide cavity as shown in Fig. 11. The advantage of this design is that a large coupling efficiency between the LED and an optical fiber can be achieved (20).

Lasers. The edge emitting LED can be extended a bit further by exploiting the natural reflectivity of the facets and increasing the lateral confinement to produce a waveguide laser. In this configuration, due to the feedback of the structure, the emission tends to be highly coherent, narrow linewidth, and highly directional. The operating principles of the semiconductor lasers are very similar to that of the LED, with the exception that in the laser, the output is coherent and is dominated by stimulated emission. Waveguide lasers adhere to the Einstein relations in that in equilibrium,

$$N_1\rho_\nu B_{12} = N_2\rho_\nu B_{21} + N_2 A_{21} \tag{13}$$

where $N_{1,2}$ is the atoms per unit volume in the collection with energy $E_{1,2}$, ρ_ν is the energy density at frequency ν, and B_{12}, B_{21}, and A_{21} are called Einstein coefficients. With appropriate math, Eq. (13) can be simplified to give the ratio of spontaneous emission to stimulated emission,

$$R = \frac{A_{21}}{\rho_\nu B_{21}} = \exp\left(\frac{h\nu}{k_B T}\right) - 1 \tag{14}$$

For example, it is apparent from Eq. (14) that for a tungsten lamp operating at 1000 K and at 10^{14} Hz, most of the emission is spontaneous and therefore highly incoherent.

When deriving the threshold conditions for a semiconductor laser, it is easiest to deal with the simplest type of semiconductor laser, the Fabry–Perot laser which is fabricated by cleaving the two ends of a semiconductor waveguide. Figure 12 shows a simple schematic of a Fabry–Perot type laser. In this case, we can determine the threshold gain by considering the beam intensity as it travels one complete round trip through the cavity. When the beam travels from one end facet to the other, it will have a beam intensity given by

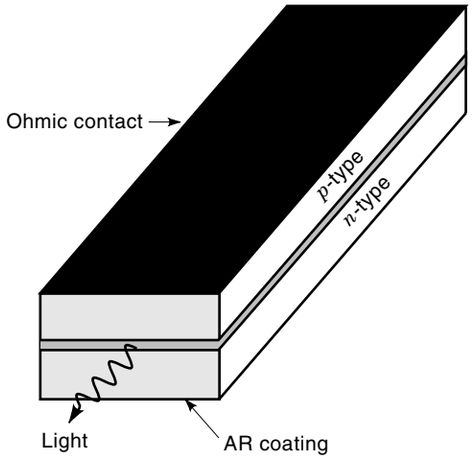

Figure 11. Light emitting diode (LED) structure sandwiched in a waveguide cavity. The shaded portion indicates the depletion region.

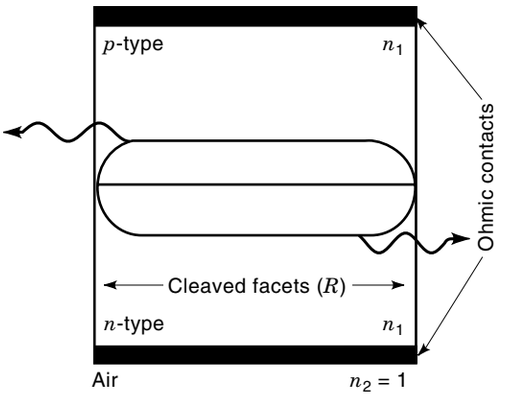

Figure 12. A cross section of a simple Fabry–Perot type laser structure. The feedback occurs between two cleaved facets with reflectivity (R).

$$I = I_0 \exp\left((k_{th} - \gamma)L\right) \tag{15}$$

where k_{th} is the threshold gain coefficient, γ is a term that incorporates all the inherent losses in the semiconductor material, L is the length of the waveguide, and I_0 is the initial intensity. After the laser reflects from the second mirror, it will have an intensity given by

$$I = RI_0 \exp\left((k_{th} - \gamma)L\right) \tag{16}$$

Finally, after making a complete round trip, the gain, which is the final intensity divided by the initial intensity is given by

$$G = R^2 \exp\left(2(k_{th} - \gamma)L\right) \tag{17}$$

If the G is greater than unity, then the oscillations will grow without bound, while if G is less than unity, the oscillations will be damped. For lasing to occur, G is set to unity,

$$G = 1 = R^2 \exp\left(2(k_{th} - \gamma)L\right) \tag{18}$$

in which case, Eq. (18) transforms to

$$k_{th} = \gamma + \frac{1}{2L}\ln\left(\frac{1}{R^2}\right) \tag{19}$$

where

$$R = \left(\frac{n_1 - n_2}{n_1 + n_2}\right)^2 \tag{20}$$

There are a number of variants of the waveguide laser that modify the lasing medium to enhance the performance. Some

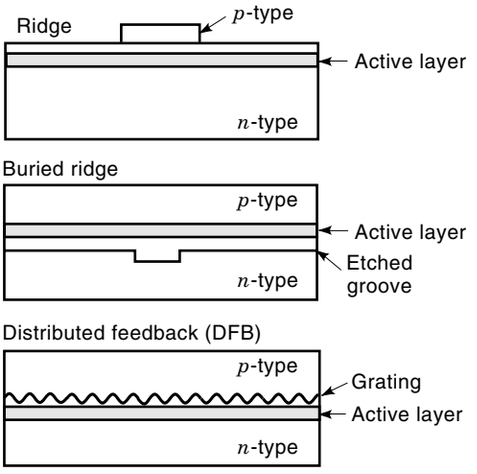

Figure 13. Common semiconductor laser structures.

of these variants are shown in Fig. 13 and are described in more detail elsewhere (21).

Amplification

Optical amplifiers are an integral element in fiber optic communication systems. These devices directly amplify the optical signal without the need for an intermediate optical to electrical conversion typical of most repeater stages. The type of amplifier to be discussed in this section is the semiconductor laser amplifier (SLA), which is not to be confused with the Erbium doped fiber amplifier (EDFA). The SLA is an entirely semiconductor device. The underlying principles of this device are very similar to the semiconductor laser in that both devices involve the stimulated emission of radiation. The difference, though, is that the feedback inherent in a laser is suppressed in the SLA. The "gain" in the SLA is due to the fact that a population inversion, similar to the laser, is created, and the incoming signal is amplified by stimulating the carriers to recombine.

SLAs can be classified into two categories, resonant and nonresonant. An example of the resonant type SLA is the Fabry–Perot amplifier (FPA). This device, in its simplest form, is a conventional waveguide laser biased slightly below its lasing threshold. In the FPA, the gain is achieved when the signal is amplified through multiple passes through the gain medium. The advantage of this device is its simplicity and the considerable gain available at the resonant frequency; the disadvantages, however, are its need for frequency matching and the concomitant narrow bandwidth. An example of a nonresonant SLA is the traveling wave amplifier (TWA). The TWA achieves gain through a single transmission through the gain medium. The TWA is the more commonly used structure since it exhibits higher gain bandwidth, higher gain saturation, and lower noise figure. The disadvantage of this type of device is the need for high quality antireflection coatings at the end facets. This increases the processing complexity of the device. Figure 14 shows a schematic of the operation of the resonant and the nonresonant types of SLAs (22).

Detection

In every practical system, there needs to be at least one conversion from the optical domain into the electrical domain. The optical detector functions in this role. A variety of optical detectors can be integrated with waveguide components. This section does not deal with the aspects of detection and detector types, but instead considers the advantages of waveguide integration and the methods of integrating the waveguide components with the detectors.

Advantages. The advent of complex telecommunication networks such as wavelength division multiplexing, coherent detection, regenerators, and so on, has resulted in an increase in the number of optical and optoelectronic devices. The deployment of these devices requires extremely reliable and low cost systems. By integrating the detection function with the waveguides, the need to connect a detector in a hybrid fashion is alleviated, which results in a savings in packaging costs, a more robust package, and enhanced performance due to less extrinsic loss. These advantages clearly are not mutually exclusive, with the manufacturing and performance issues directly affecting the cost. Good design criteria must be implemented to balance all of these parameters to create a viable integration (23,24).

The photocurrent in a detector is given by

$$I_{\text{ph}} = \eta P_{\text{inc}} \frac{\lambda}{1.24} \tag{21}$$

where P_{inc} is the incident optical power, λ is the wavelength in micrometers, and η is the quantum efficiency defined by

$$\eta = \eta_{\text{int}} \eta_{\text{ext}} \tag{22}$$

where η_{int} is a measure of the number of electron-hole pairs created for each incident photon. In most materials this num-

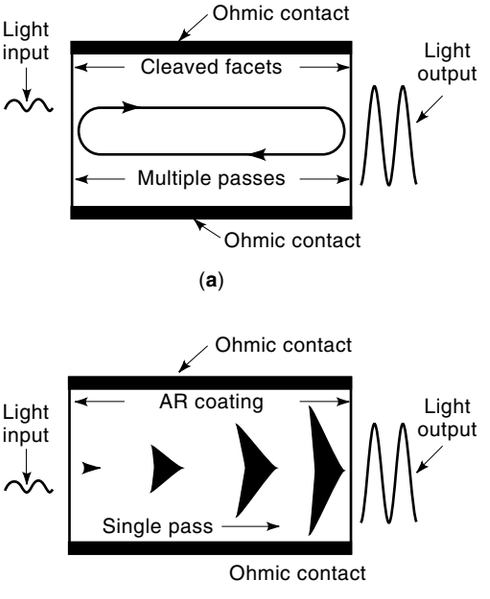

Figure 14. Semiconductor laser amplifiers (SLA). (a) In resonant mode. (b) In nonresonant mode.

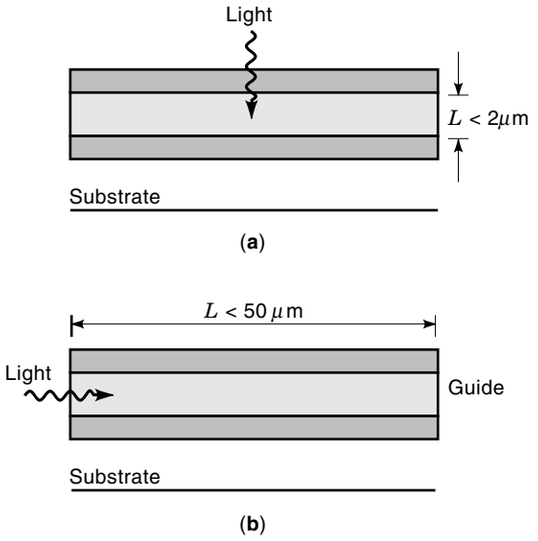

Figure 15. Photodetectors (a) In vertical mode. (b) In waveguide mode.

ber can be treated as unity. The external quantum efficiency is given by

$$\eta_{\text{ext}} = R[1 - \exp(-\alpha L)] \tag{23}$$

where R is the reflection coefficient, α is the absorption coefficient, and L is the device length. In an integrated form, R can be treated as unity without the need for expensive and intricate antireflection coatings. Typical absorption coefficients are on the order of 10^3 cm^{-1}, in which case, to achieve a 50% efficiency, the device would have $L \geq 0.7$ μm. While this is readily attainable in standard detectors, the true performance advantages become apparent when considering the reflections and when considering higher frequency limitations. Similarly, it is very easy to design a waveguide detector

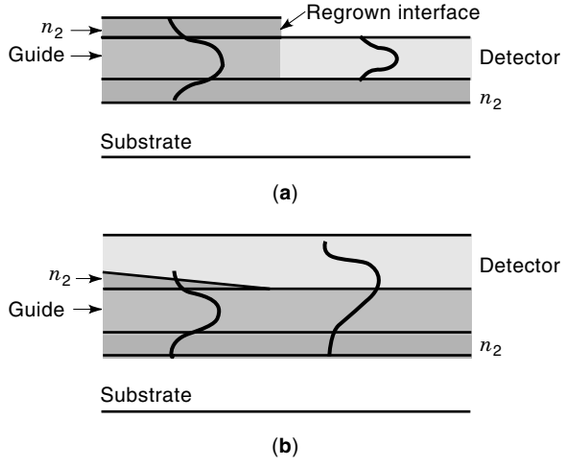

Figure 16. Waveguides integrated with photodetectors by the end-fired method. (a) Detection region is placed adjacent to the waveguide. (b) Detection region is placed atop a constricted (tapered) waveguide. In both cases, the guided light is coupled from the waveguide on the left to the detector on the right.

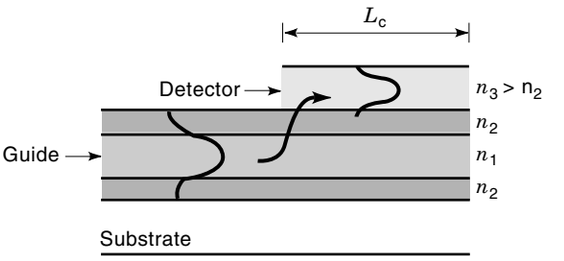

Figure 17. Cross section of a vertically coupled waveguide photodetector. In this scheme, the guided light is coupled vertically through a coupling process described earlier and is subsequently absorbed in the detector portion.

such that L is extremely large since it is defined by the waveguide length and not by the material thickness. This effectively decouples the effect of device length L from the bandwidth. The important dimensions of a vertical and waveguide photodetector are shown in Fig. 15.

Integration. There are two methods of integrating the detection function with the waveguide. The first of these is by end-fired coupling the detector with the waveguide. This may take on several forms, but the physical description is similar for the variants. The second method is for the detector to absorb the propagating light through some form of directional coupling. End-fired coupling and its variants are shown in Fig. 16. The advantage of this type of coupling is high efficiency coupling that leads to smaller devices, and subsequently to higher frequency devices. The disadvantage of this type of structure is in its complex fabrication process. The second method uses directional coupling to couple into a waveguide portion of the waveguide. The advantage of this type of structure shown in Fig. 17 is that it entails a simpler fabrication scheme, the disadvantage though is that it entails more complex initial design and longer devices which are determined by the coupling ratio and the coupling length.

OPTICAL WAVEGUIDE MODULATORS AND SWITCHES

Among the non-light-emitting active optical waveguide components, waveguide modulators and active waveguide distributors (also referred to as switches) are the most commonly used active devices which provide guided-wave control by an external electric bias or other perturbation. There are three types of optical waveguide modulators: phase modulator, amplitude (intensity) modulators, and polarization modulators. Waveguide distributors or switches can be generalized as $N \times M$ switches for which N is the number of input port and M is the number of output ports. There are different types of switches as well, such as light power switches, wavelength switches, phase or polarization switches, and so on.

Optical Waveguide Phase Modulators

To induce a phase shift on a lightwave propagating in an optical waveguide, one needs to modulate the refractive index tensor in the waveguide material with an external perturbation, such as an electric field. The phase change is given by $\Delta\varphi = \Delta\beta l = (2\pi\Delta n/\lambda)l$, where Δn is the change of the refrac-

tive index. The wavelength, λ, and the length of the modulator, l, are fixed. Many physical effects are involved in refractive index changes. The most commonly used electric bias induced effects are linear electrooptic effect, electrorefractive effect, quantum confined Stark effect, band-filling effect, and plasma effect. In general, these effects may coexist under an external electric field, but more often, one of the effects dominate. There are other effects such as acousto-optic, magneto-optic, and thermo-optic which have also been used for waveguide devices. These devices are not commonly used and will be discussed in a later section titled Other Waveguide Devices.

Electro-Optic Phase Modulator. Linear electro-optic effect (25), also known as the *Pockel's effect,* is related to the biaxial birefringence induced by an external electric field which distorts the original electron distribution in the crystal lattice. This biaxial birefringence exhibits a variation of the index in both the ordinary and extraordinary ray directions which is linearly proportional to the external field. The linear electro-optic effect can be expressed as:

$$\Delta\left(\frac{1}{n^2}\right)_i = \sum_{j=1} r_{ij}E_j^e \qquad i = 1, \ldots, 6; \qquad j = 1, 2, 3 \tag{24}$$

where n is the index, E_j^e is the electric field in j direction, and r_{ij} is the linear electro-optic tensor or simply the electro-optic coefficient. Linear electro-optic coefficients of some commonly used crystals are given in Refs. 10 and 25. Since the index change is very small in the electro-optic effect, Δn is approximately proportional to the electric field. A typical example of a linear electro-optic phase modulator is a $LiNbO_3$ waveguide modulator. $LiNbO_3$ has $n_x = n_y = n_o$ (for ordinary rays) and $n_z = n_e$ (for extraordinary rays). If the waveguide is fabricated for light propagating in the x-direction and the electric field is applied in the z-direction, as shown in Fig. 18, the change of indices for the y-polarized (ordinary) and z-polarized (extraordinary) rays, respectively, can be deduced from Eq. (24) as:

$$\Delta n_o = \frac{1}{2}r_{13}n_o^3E_z^e; \qquad \Delta n_e = \frac{1}{2}r_{33}n_e^3E_z^e \tag{25}$$

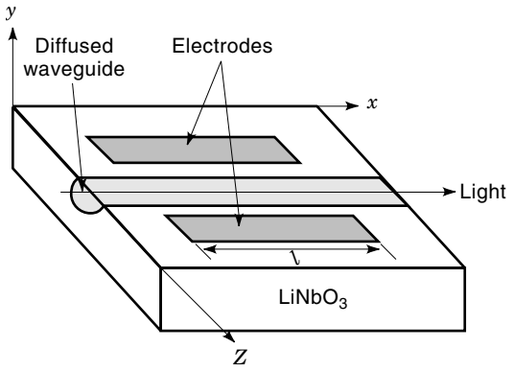

Figure 18. $LiNbO_3$, y-cut, x-propagating, waveguide modulator. The diffused embedded strip waveguide is parallel to the x-axis. Two strip electrodes of length l are located on each side of the waveguide such that the bias is applied in the z direction.

For a waveguide device with a total length l, thickness d, and applied bias V, the phase shift for z-polarized light (TM) and y-polarized light (TE) are:

$$\Delta\varphi_z = -\frac{1}{2}k_0n_e^3r_{33}\frac{V}{d}l \qquad \Delta\varphi_y = -\frac{1}{2}k_0n_o^3r_{13}\frac{V}{d}l \tag{26}$$

respectively. Where $k_0 = 2\pi/\lambda$. Since $r_{33} = 30.9 \times 10^{-12}$ m/V and $r_{13} = 9.6 \times 10^{-12}$ m/V for $LiNbO_3$, the phase shift is polarization dependent. The voltage needed for a π phase rotation is called the half-wave voltage V_π:

$$V_\pi = \frac{\lambda d}{n_e^3r_{33}l} \qquad (z\text{-polarization}) \tag{27}$$

Electrorefractive and Quantum Well Phase Modulators. The complex dielectric function ϵ (or the refractive index n, $\epsilon = (n + ik)^2$) is a function of a transition frequency ω_j (26):

$$\epsilon(\omega) = 1 + \frac{4\pi e^2}{m}\sum_j \frac{D_N f_j}{(\omega_j^2 - \omega^2) - i\Gamma_j\omega} \tag{28}$$

where e is the electron charge, m is the electron effective mass, D_N is the density of electrons, f_j is the quantum mechanical oscillator strength for jth transition, ω is the operation light frequency, and Γ_j is a broadening parameter related to the lifetime of jth transition. In the case of a bulk semiconductor waveguide modulator, ω_j is related to the energy bandgap E_g, (ωj $= E_g/\hbar$). When an external electric field is applied, the band gap will be shifted due to the Franz–Keldysh effect (27), therefore, the index of refraction will also be changed according to Eq. (28). This effect is sometimes called the electrorefractive effect. From Eq. (28), we can see that the change of the refractive index is at a maximum near the bandgap, but the absorption loss is also very large for light energy close to the bandgap. However, if the light energy is very small compared to the band gap, the change of index becomes a minimum. Therefore, this type of waveguide is designed for an operating light energy less than but relatively close to the bandgap.

Semiconductor quantum well (QW) (28) waveguide modulators have a multiple QW structure which forms the active waveguide region. This type of device exhibits better performance than a bulk device because (a) the bias-induced change of the transition energy is more efficient than for a bulk device, due to the large quantum confined Stark shift (28,29), and (b) due to the exciton effect, the absorption edge is sharper than that of the bulk, therefore absorption loss is less. The QW waveguide device is usually polarization dependent due to the heavy-hole (HH) and light-hole (LH) valence-band split by the quantum confinement or the strain in the QW as described in Refs. 28, 30, and 31.

Phase Modulators Using Band Filling Effect and Plasma Effect. Another type of semiconductor waveguide phase modulator uses modulation doped multiple QWs in the active region. The QW is filled by two-dimensional free electron gas. The absorption edge is then defined by the Fermi energy instead of the band gap (32). When an external electric field is applied, band bending occurs in both the QW and barrier region, causing a transfer of free electrons from the QW to its ionized parent donor region in the barrier, subsequently neu-

tralizing those donors. As the number of free electrons decreases, the Fermi-level changes; therefore, the refractive index changes due to the change in the transition energy (33). This is referred to as the *band-filling effect.* When there is a change in the free carrier concentration in a semiconductor, there is another effect, plasma effect, which can also change the index of refraction (11). The free carriers have a negative contribution to the index of refraction which is analogous to the index change produced by a plasma of charged particles in a dielectric (11):

$$\Delta n = -\frac{\omega_p^2}{2n\omega^2} = -\frac{Ne^2}{2n\epsilon_0 m^* \omega^2} \tag{29}$$

where ω_p is the plasma frequency, m^* is the effective mass, and N is the number of free carriers. The plasma effect and the band-filling effect occur simultaneously in the QW region of the waveguide. The plasma effect can also occur in the doped cladding region in the waveguide when the bias changes the depletion near the core/cladding interface.

To enhance these effects, a barrier reservoir and QW electron transfer structure (BRAQWETS) is used as the active layer to make waveguide phase modulators. As described in Ref. 33, the electron reservoir in the barrier and the QW are built in an *i–n–i–p–i*, layer sequence for each BRAQWETS period. A bias in one direction can pour the electrons from the reservoir into the QW. Conversely, a bias in the opposite direction can recapture the electron from the QW in the *n*-type reservoir.

Optical Waveguide Polarization Modulators

$LiNbO_3$ TE-TM Mode Conversion Device. Figure 19 shows a $LiNbO_3$ based *x*-cut, *y*-propagation, TE-to-TM polarization conversion device. When an external electric field, E_y^e, is applied in the *y*-direction, an off-diagonal element, $\delta\epsilon_{yz}$, in the dielectric tensor will be created by the electro-optic effect with the off-diagonal electro-optic coefficient (EO) r_{51}, causing a coupling between the TE and TM modes. It can be shown that

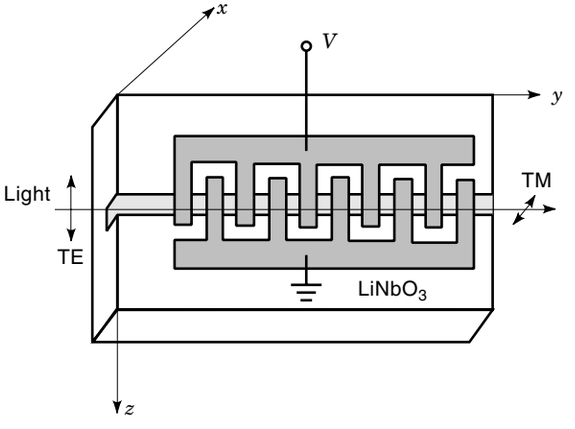

Figure 19. $LiNbO_3$, *x*-cut, *y*-propagating, TE–TM polarization conversion waveguide device. Two conjugated multiple-gated electrodes are located on top of the waveguide such that a periodic electric field can be applied along the *y*-propagating direction. By choosing a right period, bias, and device length, complete TE–TM conversion can be performed.

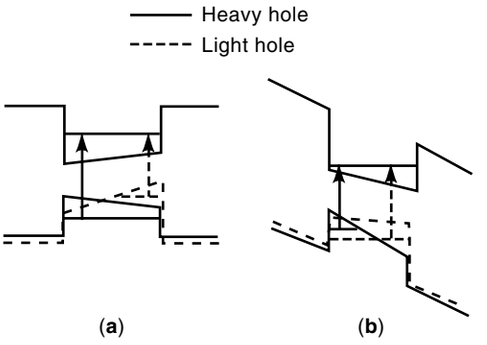

Figure 20. Band structure of the Variable-strain quantum well. (a) Without external field, the LH transition energy(dashed arrow) is smaller then the HH one(solid arrow). (b) With an external field, the HH transition energy is smaller.

a TE polarization variation, δP_z, for the extraordinary ray is produced by the *y*-component of the electric field, E_y of the TM polarized light (ordinary ray), and the applied electric field (10):

$$\delta P_z = \epsilon_0 \delta\epsilon_{yz} E_y = -\epsilon_0 n_o^2 n_e^2 r_{51} E_y^e E_y \tag{30}$$

In order to exchange optical power between the TE and TM guided mode, a phase-matching condition between the two modes has to be satisfied. Since the electro-optic effect also produces a birefringent phase shift, the electric field has to be applied in a periodic fashion such that alternate EO gating along the *y*-light-propagation direction is used to make the phase compensations as shown in Fig. 19. By choosing a right period, device length, and bias, a complete TE–TM mode conversion can occur.

Semiconductor Variable-Strain Quantum Well Waveguide with Tunable Polarization. A variable-strain QW structure was designed for semiconductor waveguide polarization modulators (34). Variable-strain QWs have a linear composition change as well as a lattice mismatch change in a semiconductor QW. As shown in Fig. 20 the heavy hole (HH) and light hole (LH) band edges have mutually opposite slopes (built-in fields) due to the linear variation of the strain in the QW. When an external bias is applied, the change of the net field for the HH band is opposite in direction to that of the LH band. As a result, there is a simultaneous blue shift in LH transition and a red shift in HH transition due to the decrease and increase of the quantum confined Stark effects, respectively (or reverse). Under certain conditions, the HH and LH band may crossover. Since the HH and LH transitions respond primarily to TE and TM polarized light, respectively, in the waveguide configuration with [001] substrate crystal orientation, a polarization modulator can be made using these variable strain QW structure in the active waveguide region.

Waveguide Polarization Rotators. Since many crystalline waveguide materials are birefringent, the polarization of linearly polarized incident light, not parallel to one of the principle crystal axes, can be rotated by the waveguide. Therefore, with use of a waveguide phase modulator with such a material, a tunable polarization rotator can be made. However, in

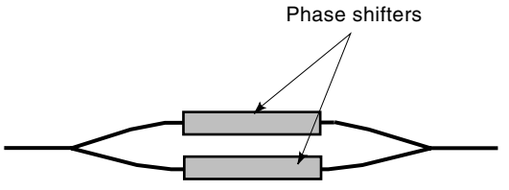

Figure 21. A typical Mach–Zehnder waveguide intensity modulator. Two phase shifters are formed on the two separated waveguide branches by introducing the electrodes and electrical isolation from other parts of the waveguide. The phase modulation may cause a constructive/destructive interference at the output port, resulting in an optical intensity modulation.

practice, there are some technical difficulties to arrange the polarization of the incident beam not parallel to any crystal axis of the waveguide.

Optical Waveguide Intensity Modulators

To achieve intensity modulations, different methods are employed in waveguide intensity modulators such as absorption (electro-absorption effect), interference effect (Mach–Zehnder modulator), modifying the mode cutoff condition in an asymmetric guide, cross-polarization configuration, and so on.

Electroabsorption Modulators. Electroabsorption modulators are operated near the absorption edge or the bandgap. Since the bandgap of III–V compound semiconductors such as InGaAs and InGaAsP can easily be engineered to match the waveguide operating wavelength (0.8 to 1.55 μm), electroabsorption modulators are used mostly for semiconductor waveguides with a p–i–n layer configuration. For bulk active core layer modulators, without an external field, the bandgap is above the light energy. With a reverse bias, the bandgap shifts due to the Franz–Keldysh effect and falls below the light energy and becomes absorbing. For multiple QW active core layer modulators, the absorption edge of the confined excitonic transition can be more efficiently red shifted with the bias due to the quantum confined Stark effect. The QW device has less loss than the bulk device due to the sharper absorption edge. More details on these electroabsorption effects can be found in Refs. (28) and (29).

Mach–Zehnder Modulators. Another type of waveguide intensity modulator is a Mach–Zehnder modulator which is a waveguide version of the Mach–Zehnder interferometer. There are various embodiments of Mach–Zehnder waveguide modulators; a typical one is shown in Fig. 21, where the guided beam is split into two uncoupled waveguide channels, a phase shifter is incorporated in each channel (sometimes only in one channel), and the two channels then recombine into the output waveguide where constructive/destructive interference occurs. If the phase is shifted periodically between 0 and π, the output light intensity will oscillate between maximum and minimum power. Basically, Mach–Zehnder modulators convert a phase modulation into an intensity modulation.

Other Intensity Modulators. There are a number of less common intensity modulators. For example:

1. Asymmetric waveguides modulated with optical mode cut-off (10), where the device is designed such that without bias, the index difference between an asymmetric cladding/core/cladding layers is just below the critical value to support the fundamental mode. Applying an appropriate voltage, the index increment is increased above the cut-off point so that the guided mode can be supported and transmitted.
2. Intensity modulation by transverse polarization (10). Intensity modulation can be made by a combination of a waveguide birefringent phase modulator sandwiched between crossed polarizers. Intensity modulation can be also made by a waveguide polarization modulator and polarizer (analyzer) combination.
3. Intensity modulation by varying the coupling efficiency. This type of modulator is similar to the optical waveguide power switch.

Issues of High Speed On/Off Modulation and Polarization Insensitivity. As mentioned in opening section, high speed modulation and polarization insensitivity are very important issues for large bandwidth communication and optically controlled microwave applications. Since the speed for an external modulator is limited by the device capacitance, reducing the capacitance requires minimizing the device size. Semiconductor multiple QW electroabsorption modulators are the best candidates, because they have high modulation efficiency, only 50 to 100 μm of length is needed for a modulator monolithically integrated with a passive waveguide (12,13). Ultra high-speed modulation up to 50 GHz have been reported using these types of devices (13). Another advantage of the semiconductor QW waveguide is that by introducing tensile strain or δ-strain layers in the QW to make the HH and LH levels degenerate, polarization insensitivity can be achieved in the waveguide device (13,31).

Optical Waveguide Switches and Active Distribution Network

Directional Coupling Power Switches. There are several types of optical waveguide power switches. The most commonly used is the directional coupler switch. A directional coupler is formed by placing two waveguides in close proximity, as shown in Fig. 8. The power distribution between the two guides depends on both the coupling coefficient and the propagation synchronization ($\Delta\beta$) as described earlier. Power switching occurs by placing a phase modulator on each guide to change the synchronism (the relative difference of the propagation constants $\Delta\beta$) (19). This type of switch has been made in both $LiNbO_3$ and III–V semiconductors, and exhibits high extinction ratio with relatively low bias voltages (35,36). $1 \times N$ and $N \times N$ switching matrices can be made by combining the 2×2 coupling switches. These matrix switches are in great demand for fiber communication systems.

Polarization, Interferometric, and Intersecting Waveguide Switches. A polarization switch can be made by combining a Y-branch splitter with two polarization modulators on each of the branches. TE or TM polarized input beams will be discriminated by polarization on each of the polarization modulators that has independent on/off control for TE (or TM) mode propagation. With use of the same principle, a 2×2 switch can be made by combining two Y-branch polarization switches as described above such that a two input/two output cross switch is configured.

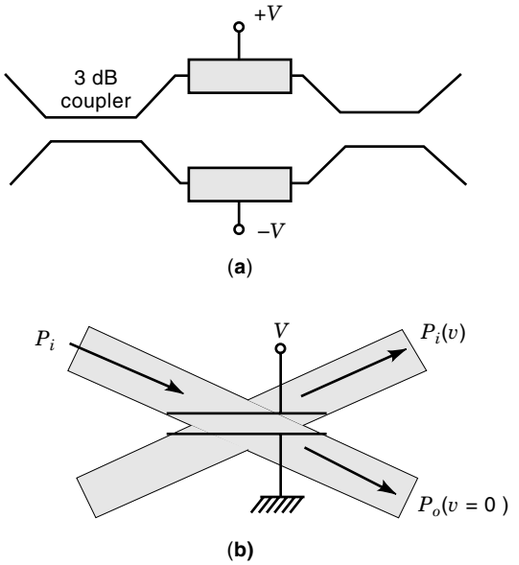

Figure 22. (a) Mach–Zehnder waveguide interferometric switch. (b) Intersecting waveguide switch.

The interferometric switch (also called balanced-bridge interferometric switch) is another form of Mach–Zehnder waveguide modulator, in which the single input/output of the regular Mach–Zehnder waveguide is replaced by a double inputs/outputs with a 3 dB directional coupler as shown in Fig. 22(a). The power distribution of the two outputs can be controlled by the phase-shifters in the Mach–Zehnder waveguide channels. More details can be find in Ref. 19.

Another type of switch uses the x-intersecting-waveguide configuration (19). As shown in Fig. 22(b), a pair of parallel electrodes are placed on the intersection along the line of symmetry. At zero bias, the incident guided modes can pass straight through the intersection. With an appropriate voltage, the incident light reflects from the edge of the electrode into the crossed waveguide due to total internal reflection caused by the index changes between the two electrodes.

Digital Optical Switches. A digital optical switch (DOS) uses the mode evolution principle (37) in a weakly coupled Y-branch switch (38,39) instead of a mode interference principle used in directional coupler switches or Mach–Zehnder switches. The switching state of DOS exhibits a threshold value in its control parameter, beyond which the switch remains in a 1/0 constant state. This type of switch is of interest for optical communication networks because it has a high extinction ratio, polarization, and wavelength (within a certain range) insensitivity (38,39).

Wavelength Switching for Wavelength Division Multiplexing. Wavelength switching is one of the key functions needed for WDM networks. There are several optical waveguide wavelength switching devices. One is a combination of passive N-channel phased-array waveguide grating device with an active $N \times N$ switching network as mentioned earlier. As described in the Refs. 40 and 41, the phased-array waveguide grating can distribute an N-color incident beam into N separate output channels according to the sequence of their wavelengths. Then, the $N \times N$ star network can dynamically switch the N wavelength outputs in any given order.

Another type of waveguide wavelength switching device is based on tunable wavelength filtering such as tunable Mach–Zehnder filters and tunable Fabry–Perot filters. The details of these devices are given in Ref. 42 for Mach–Zehnder filters and Ref. 43 for Fabry–Perot filters. These filters involve thermo-optic effects and acousto-optic effects, which are both discussed in the next section.

Other Waveguide Devices

In this section, we discuss other discrete waveguide components, including acousto-optic, magneto-optic and all-optical devices. These active devices utilize different effects to change their refractive indices and thus cause their state to be altered, each method having their own advantages and disadvantages.

Acousto-Optic Devices. Acousto-optic effect provides an important means of optical wave control and is implemented in various functional devices. When an acoustic wave propagates in an optically transparent medium, it produces a periodic modulation of light via the elasto-optic effect (44), which describes the change of refractive index of the optical medium due to the acoustic wave. In materials where the birefringent effect is large, there is an additional effect due to the antisymmetric rotation of the deformation gradient (45). Further, in piezoelectric crystals an indirect elasto-optic effect occurs as a result of the piezoelectric effect and the electro-optic effect in succession (46). The traveling sound wave that produces the acousto-optic effect can be transverse, longitudinal, or a combination of the two, as in surface acoustic waves (SAW). Since a SAW and a guided optical wave are each restricted to a thin surface layer with a thickness on the order of their wavelengths, they are spatially well matched, their energy densities are high, and it is possible to have efficient coupling between them. A surface acoustic wave is usually stimulated by an interdigital transducer, which is produced by depositing an interdigited electrode on the surface of a piezoelectric medium. The technology to fabricate interdigital transducers is well developed and quite versatile (47). Acousto-optic guided wave devices include mode converters, deflectors modulators, switches, and tunable filters (47).

Mode converters may be implemented by coupling between two guided waves of different modes due to a collinear acousto-optic interaction between guided waves and a SAW propagating along the same direction. In isotropic waveguides, conversion of mode-order is only possible because there is no collinear coupling between modes of different polarization. Additionally, in anisotropic waveguides, TE–TM mode conversion, as well as mode-order conversion, is possible because the off-diagonal components of the dielectric tensor are nonzero. Mode converters have been fabricated in various waveguide material systems. These systems include mode-order conversion in glass film waveguides deposited on an Al reflection layer on a $LiNbO_3$ substrate (48), sputtered ZnO film waveguides on a fused quartz substrate (49), and TE–TM mode conversion in Ti-diffused $LiNbO_3$ waveguides (50).

Acousto-optic tunable filters are optical wavelength filters where the center optical wavelength of the filter pass-band can be tuned by varying the SAW frequency. The first such

device was proposed by Harris and Wallace (51) and was configured so that the interacting optical and acoustic waves were collinear. In the guided wave devices, the tunable wavelength range is limited mainly by the SAW transducer excitation bandwidth. A very narrow filter bandwidth can be achieved with a moderate length by optimizing the high-index cladding thickness. Most of the devices use single waveguides, but a multilayered two waveguide directional coupler has been proposed and demonstrated (52).

Modulators, switches, and deflectors can be implemented utilizing coplanar acousto-optic diffraction; they are called waveguide Bragg cells. The diffraction efficiency and the direction angle are controlled by the SAW power and frequency, respectively. The SAW power is the RF power fed to the SAW transducer, multiplied by the transducer conversion efficiency. Many waveguide modulators and switches have been reported (47). Materials with large acousto-optic constants such as As_2S_3 on Y-cut $LiNbO_3$ (53) require a reduced RF power. Single material waveguides fabricated on a piezoelectric substrate are advantageous and the material most commonly used for such devices has been $LiNbO_3$, with LiO_2 outdiffusion or Ti in-diffusion for the waveguides; however, GaAs and related III–V semiconductor materials have been used more extensively in recent years.

In view of future OEIC implementation, the most favorable substrate materials are, of course, silicon, InP, and GaAs. If the waveguide film is not piezoelectric a transducer must be fabricated by deposition of a piezoelectric film on a portion of the substrate (54). Devices have been fabricated using $As_2S_3/SiO_2/Si$; glass/SiO_2/Si; Si_3N_4/SiO_2/Si and InP or GaAs waveguides (47).

Acousto-optic interaction can be used to deflect an optical beam in a sequential or random access manner. For such an application, the bandwidth and the time bandwidth product should be maximized to obtain a large deflection angle region and a large number of resolvable parts. Many such devices have been reported using Ti-diffused or outdiffused $LiNbO_3$ waveguides (55). Wide bandwidths have been achieved through modifications of the transducer and the use of anisotropic Bragg diffraction.

Magneto-Optic Devices. Magneto-optical waveguide devices are based on magneto-optical interactions between optical guided waves and magnetostatic waves (MSW) in magnetic substrates, the archetypal being Yttrium Iron Garnet–Gadolinium Gallium Garnet (YIG–GGG) which is transparent in the infrared. MSW can be generated by applying a RF signal. The moving optical gratings induced by the MSW cause a magneto-optic interaction via the Faraday and Mouton–Cotton effects (56). Thus, guided wave Bragg cell magneto-optical devices can be made analogous to acousto-optic devices. The advantage of magneto-optic devices is that they provide a unique nonreciprocity that can be implemented in nonreciprocal devices such as isolators and circulators (57,58). Recent improvements in fabrication and ion milling have allowed the realization of integrated magneto-optical modules. In YIG/GGG waveguides the Faraday rotation angle per unit length is limited by the saturation of the magnetization and phase matching must be incorporated in TE–TM mode converters. TE–TM degenerate waveguides, required for phase matching in nonreciprocal mode converters, and (Ga,Sc) substituted YIG waveguides on GGG substrate magneto-optic modulator/switches have been demonstrated (59). High speed wideband integrated magneto-optical frequency shifters and modulators have also been demonstrated (60–62).

Nonlinear All-Optical Devices. Nonlinear optical effects based on the χ^2 and χ^3 nonlinearities in optical waveguides have been intensively studied from the very beginning of integrated optics (63–67). Materials for guided-wave optical nonlinear applications have to exhibit large nonlinearities, be suitable for waveguide fabrication, and be capable of phase matching. $LiNbO_3$ has been the material system of choice for these devices. Difference frequency generation and frequency conversion has been demonstrated in these devices. Bistable all-optical waveguide devices have also been demonstrated in both GaAs and $LiNbO_3$ systems. Other waveguide devices such as Mach–Zehnders and directional couplers have also been reported. However, these devices, as well as their response times, are long, and high-density integration is difficult.

BIBLIOGRAPHY

1. P. E. Green, Jr., *Fiber Optic Networks,* Englewood Cliffs, NJ: Prentice-Hall, 1993, and references cited in.
2. N. S. Kapany, *Fiber Optics Principles and Applications,* New York: Academic Press, 1967.
3. D. B. Anderson, *Optical and Electro-optical Information Processing,* 221, Cambridge, MA: MIT Press, 1965.
4. N. S. Kapany and J. J. Burke, *Optical Waveguides,* New York: Academic Press, 1972.
5. D. Marcuse, *Light Transmission Optics,* Princeton, NJ: Van Nostrand Reinhold, 1972.
6. R. N. Hall et al., *Phys. Rev. Lett.,* **9**: 366–367, 1962.
7. R. N. Hall, *IEEE Trans. Electron Dev.,* **ED-23**: 700–704, 1976.
8. A. Yarive and R. C. C. Leite, *Appl. Phys. Lett.,* **2**: 57–59, 1963.
9. S. E. Miller, *Bell Syst. Tech. J.,* **48** (7): 2059, 1969.
10. H. Nishihara, M. Haruna, and T. Suhara, *Optical Integrated Circuits,* R. E. Fischer and W. J. Smith (eds.), New York: McGraw-Hill, 1987.
11. R. G. Hunsperger, *Integrated Optics: Theory and Technology,* T. Tamir (ed.), Berlin: Springer-Verlag, 1985.
12. O. Mitomi et al., *Appl. Optics,* **31**: 2030–2035, 1992.
13. T. Ido et al., *IEEE, J. Light. Tech.,* **14**: 2026–2034, 1996.
14. C. A. Brackett, *IEEE J. Selec. Area. Commun.,* **8**: 948, 1990.
15. C. W. Pearce, *Epitaxy,* A. C. Adams, *Dielectric and Polysilicon Film Deposition,* J. C. C. Tsai, *Diffusion,* T. E. Seidel, *Ion Implantation,* D. A. McGillis, *Lithography,* C. J. Mogab, *Dry Etching,* and W. Fichtner, *Metallization.* In *VLSI Technology,* S. M. Sze (ed.), New York: McGraw-Hill, 1983.
16. H. Kogenlnik, Theory of dielectric waveguides. In *Integrated Optics,* T. Tamir (ed.), Berlin: Springer-Verlag, 1979.
17. B. E. A. Saleh and M. C. Teich, *Photonics,* New York: Wiley, 1991, pp. 238–271.
18. R. Marz, *Integrated Optics,* Boston: Artech House, 1995, pp. 77–217.
19. T. Tamir et al., *Guided-Wave Optoelectronics,* Berlin: Springer-Verlag, 1988, pp. 96–144.
20. H. Kressel and J. K. Butler, *Semiconductor Lasers and Heterojunction LEDs,* New York: Academic Press, 1977.
21. G. P. Agrawal and N. K. Dutta, *Long Wavelength Semiconductor Lasers,* New York: Van Nostrand Reinhold, 1986.

22. T. Saitoh and T. Mukai, *Traveling-Wave Semiconductor Laser Amplifiers, Coherence, Amplification, and Quantum Effects in Semiconductor Lasers,* New York: Wiley, 1991.
23. R. J. Deri, Monolithic integration of optical waveguide circuitry with III-V photodetectors for advanced lightwave receivers, *IEEE J. Lightwave Technol.,* **11**: 1296, 1993.
24. A. Alping, Waveguide pin photodetectors: theoretical analysis and design criteria. *IEE Proc.,* **136** (Pt. J): 177, 1989.
25. A. Yariv, *Optical Electronics,* 3d Ed., New York: Holt, Rinehart and Winston, 1985.
26. F. Wooten, *Optical Properties of Solids,* New York: Academic Press, 1972.
27. J. I. Pankove, *Optical Processes in Semiconductors,* Englewood Cliffs, NJ: Prentice-Hall, 1971.
28. G. Bastard and J. A. Brum, *IEEE J. Quantum Electron.,* **22**: 1625, 1986.
29. D. A. B. Miller et al., *Phys. Rev. Lett.,* **53**: 2173–2175, 1984.
30. D. S. Chemla et al., *IEEE J. Quantum Electron.,* **20**: 265, 1984; and D. L. Smith and C. Mailhiot, *Rev. Mod. Phys.,* **62**: 173–234, 1990.
31. H. Shen et al., *Appl. Phys. Lett.,* **72** (6): 683–685, 1998.
32. K. Ploog and G. H. Dohler, *Adv. Phys.,* **32**: 285, 1983.
33. M. Wegener et al., *Appl. Phys. Lett.,* **55**: 583–585, 1989; J. E. Zucker et al., *Appl. Phys. Lett.,* **56**: 1951, 1990.
34. W. Zhou et al., *Appl. Phys. Lett.,* **66**: 607, 1995.
35. R. V. Schmidt and L. L. Buhl, *Electron. Lett.,* **12**: 575, 1976; R. C. Alferness, R. V. Schmidt, E. H. Turner, *Appl. Opt.,* **18**: 4012, 1979.
36. F. J. Leonberger and C. O. Bozler, *Appl. Phys. Lett.,* **31**: 223, 1977; K. Tada et al., *Tech. Dig. 7th Topical Meeting Integrated Guided Wave Optics,* Kissimee, FL, **WB-4**: 1984.
37. W. K. Burns et al., *Appl. Opt.,* **14**: 1053–1065, 1976.
38. J. F. Winchant et al., *Electron. Lett.,* **28**: 1135–1137, 1992.
39. A. Sneh et al., *IEEE Photon. Technol. Lett.,* **9**: 1589–1591, 1997.
40. C. Dragone, C. A. Edwards, and R. C. Kistler, *IEEE Photon. Technol. Lett.,* **3**: 896, 1991.
41. W. Lin et al., *Tech. Dig. Conf. Laser Electro-Optics'96,* **9**: 344, 1996.
42. K. Nosu et al., *IEEE J. Lightw. Technol.,* **11**: 764, 1993.
43. H. Kobrinski and K-W Cheung, *IEEE Commun. Mag.,* 53–63, Oct, 1989, reference cited in.
44. L. Brillouin, *Ann. Phys.,* **17**: 80–122, 1892.
45. D. F. Nelson and M. Lax, *Phys. Rev. Lett.,* **24**: 378–380, 1970; Theory of photoelastic interaction, *Phys. Rev.,* **B3**: 2778–2794, 1971.
46. R. W. Dixon, *IEEE J. Quantum Electron.,* **QE-3**: 85–93, 1967.
47. C. S. Tsai, Guided wave acousto-optics. *Electronics and Photonics,* Berlin: Springer Series, Springer-Verlag, Vol. **23**: 1990.
48. L. Kuhn, P. F. Heidrich, and E. G. Lean, *Appl. Phys. Lett.,* **19**: 428, 1971.
49. H. Sasaki and N. Mikoshiba, *Proc. IEEE Ultrasonic Symp.,* **18**: 1979.
50. Y. Ohmachi and J. Noda, *IEEE J. Quantum Electron.,* **QE-13**: 43, 1977.
51. S. E. Harris and R. W. Wallace, *J. Opt. Soc. Am.,* **59**: 744–747, 1969.
52. N. Goto, Y. Miyazaki, and Y. Akao, *Japan J. Appl. Phys.,* **21**: 1611, 1982.
53. Y. Ohmachi, *J. Appl. Phys.,* **44**: 3928, 1973.
54. S. K. Yao, R. R. August, and D. B. Anderson, *J. Appl. Phys.,* **49**: 5728, 1978.
55. C. S. Tsai, *IEEE Trans. Circuits Syst.,* **26**: 1072, 1979.
56. C. S. Tsai and D. Young, *IEEE Trans. Microw. Theory Tech.,* **MTT-38**: 560–573, 1990 and references cited therein.
57. J. P. Castera and G. Hapner, *Appl. Opt.,* **16**: 2031, 1971.
58. T. Mizumoto and Y. Naito, *IEEE Trans. Microw. Theory Tech.,* **MTT-30**: 922, 1982.
59. P. K. Tein et al., *Appl. Phys. Lett.,* **21**: 394, 1975.
60. J. Warner, *IEEE Trans. Microw. Theory Tech.,* **MTT-23**: 70, 1975.
61. G. Hapner, B. Besormire, and J. P. Castera, *Appl. Opt.,* **14**: 1479, 1975.
62. A. Shibukawa and M. Kobayashi, *Appl. Opt.,* **20**: 2444, 1981.
63. A. Yariv, *IEEE J. Quantum Electron.,* **QE-9**: 919, 1973.
64. P. K. Tein, *Rev. Mod. Phys.,* **49**: 361, 1977.
65. H. F. Taylor and A. Yariv, *Proc. of IEEE,* **62**: 1044, 1974.
66. H. A. Haus, *Wave and Fields in Optoelectronics.* Englewood Cliffs, NJ: Prentice-Hall, 1984.
67. A. Yariv and P. Yeh, *Optical Waves in Crystals.* New York: Wiley, 1984.

WEIMIN ZHOU
HONGEN P. SHEN
JAGADEESH PAMULAPATI
U.S. Army Research Laboratory
MITRA DUTTA
U.S. Army Research Office